Nutrient and diatom dynamics during late winter and spring in the Oyashio region of the western subarctic Pacific Ocean

Koji Sugie [a, b]*, Kenshi Kuma [a, c], Satoshi Fujita [a], Yuta Nakayama [a], Tsutomu Ikeda [c]

a: Graduate School of Environmental Science, Hokkaido University, Kita 10-Nishi 5, Kita-ku, Sapporo, Hokkaido 060-0810, Japan

b: Present address: Central Research Institute of Electric Power Industry, 1646 Abiko, Abiko, Chiba 270-1194, Japan

c: Faculty of Fisheries Science, Hokkaido University, 3-1-1 Minato-cho, Hakodate, Hokkaido 041-8611, Japan

* Corresponding author
Koji Sugie
Central Research Institute of Electric Power Industry, 1646 Abiko, Abiko, Chiba 270-1194, Japan
Tel: +81-4-7182-1181, Fax: +81-4-7183-2966
E-mail: kojisugie@gmail.com

Keywords: Nutrient; Iron; spring bloom; Si:N ratio; Diatom; western subarctic Pacific Ocean

Abstract

We investigated the nutrient and diatom dynamics during late winter and spring (9-March to 1-May 2007) in the Oyashio region as part of the OECOS-WEST research cruises. Macronutrients, iron, chlorophyll *a* (Chl-*a*) and biogenic silica (BSi) concentrations in the upper mixed layer varied remarkably ranges were 1.88–18.8 μmol L^{-1} for NO_3+NO_2, 0.64–1.85 μmol L^{-1} for PO_4, 3.14–35.7 μmol L^{-1} for $Si(OH)_4$, 0.14–0.54 nmol L^{-1} for D-Fe, 0.64–24.6 nmol L^{-1} for T-Fe, 0.30–17.4 μg L^{-1} for Chl-*a*, and 0.34–14.1 μmol L^{-1} for BSi. Mixed layer depth (MLD) also varied from 8–190 m during the cruises. The growth rate of *in situ* phytoplankton communities, dominated by centric diatoms, varied in shipboard culture experiments from 0.55 d^{-1} for iron-replete to 0.14 d^{-1} for iron-limited conditions. A relationship between BSi and Chl-*a* concentrations indicates that the *in situ* diatom community in the warmer water system (>4°C) was heavily silicified, probably due to iron-limitation. The *in situ* macronutrient and dissolved iron concentrations below the MLD and estimated macronutrient concentrations during winter were negatively correlated to temperature (1–6°C), that is to the relative proportion of warm modified Kuroshio Water mixed into the colder Oyashio water system. The rate of decrease in $Si(OH)_4$ per °C increase was greater than the rates for NO_3+NO_2 and PO_4 for both *in situ* and estimated winter values. These results suggest that the spring bloom in the cold water system with high macronutrients and iron concentrations would progress rapidly and intensely, and then be terminated by nitrogenous nutrient depletion. However, the diatom bloom in warmer waters with lower macronutrients and iron concentrations would be terminated by Si- and/or iron-limitation of heavily-silicified diatoms. In the OECOS study, variation of macronutrients and iron due to the surface intrusions of several water masses and modification from different chemical conditions during winter were the most important factors regulating the progression, magnitude and probably fate of the spring phytoplankton bloom in the Oyashio region.

1. Introduction

The Oyashio is the western boundary current of the subarctic circulation in the Pacific. A large, annual spring phytoplankton bloom has been consistently observed in the Oyashio region, and its products appear to be transferred efficiently to higher trophic levels. This makes it a region of high productivity (Taniguchi, 1999; Sakurai, 2007). The water in the Oyashio region is characterized by high nutrient concentrations, nutrients supplied to the euphotic zone by strong vertical mixing during winter, as observed in other regions of the subarctic Pacific (Harrison et al., 2004). Saito et al. (2002) reported that the macronutrient concentrations during winter in the Oyashio region are approximately 1.3 times higher than those at Ocean Station Papa in the eastern subarctic Pacific. In addition, surface nitrate concentration during summer in the Oyashio region is drawn down to ~0.7 μmol L^{-1} by phytoplankton production (Kasai et al., 2001; Saito et al., 2002), while the oceanic subarctic Pacific is a High-Nutrient Low-Chlorophyll (HNLC) region (Banse and English, 1999; Tsuda et al., 2003; Boyd et al., 2004). The large annual macronutrient drawdown is one of the salient characteristics of the Oyashio region compared to other areas in the subarctic Pacific (Wong et al., 2002; Harrison et al., 2004). The large nutrient drawdown is likely supported by higher iron input to the euphotic layer in the western region compared to the eastern north Pacific (Nishioka et al., 2003, 2007; Takata et al., 2006; Nakayama et al., this issue). The supply of a large amount of bioavailable iron is one of the most probable reasons why the surface of the Oyashio region is not in the HNLC condition. However, Saito et al. (2002) suggested that two-thirds of subsurface (~20–30 m) water mass observed in the Oyashio region during summer seems to be in a condition similar to that in HNLC areas. In addition, iron concentration in the surface water of the Oyashio region is variable temporally and spatially (Nishioka et al., 2007). These variable iron concentrations and the diatom bloom phenomenon are similar to those of the coastal upwelling regimes in Pacific eastern boundary currents (Hutchins et al., 1998; Bruland et al., 2001, 2005). However, the physical and biological mechanisms controlling macronutrients and iron supply in the Oyashio region remain inadequately described, although they are important for the ecological dynamics in the region.

Previous research cruises have been conducted once a month at a maximum,

resulting in temporally and spatially variable macronutrient and chlorophyll *a* (Chl-*a*) recorded from year to year in the Oyashio region, especially in spring (Kasai et al., 2001; Saito et al., 2002). The hydrography in the Oyashio region is often complicated, and it has been called a "perturbed area" (Hanawa and Mitsudera, 1987), since it can be occupied by variable mixtures of two or three dominant water masses: Oyashio water, Coastal Oyashio Water and the Kuroshio extension. Each of those water types, when unmixed, has different chemical and physical conditions during winter and spring (Kono, 1997; Kono and Kawasaki, 1997; Oguma et al., 2008). Although this general picture is likely correct, the physical and biological processes generating the variability of nutrients and Chl-*a* concentrations in the Oyashio region are poorly understood because high-frequency observations are lacking for winter and spring. In the present study, we conducted intensive sampling at a fixed station in the Oyashio region for macronutrients, iron and Chl-*a* during late winter and spring in 2007 as part of the program Ocean Ecodynamics Comparison in the Subarctic Pacific (OECOS). In addition, we conducted phytoplankton culture experiments and measured biogenic silica (BSi) concentration to assess *in situ* diatom dynamics in the Oyashio region during the spring bloom period.

2. Methods

2.1 Sampling strategy

The OECOS cruises were conducted in the Oyashio region of the western subarctic Pacific Ocean from 8- to 14-March 2007, aboard the TS Oshoro-Maru, and from 5-April to 2-May 2007 aboard the RV Hakuho-Maru. Sampling was done for macronutrients (NO_3+NO_2 (hereafter N+N), PO_4 (P), $Si(OH)_4$ (Si)), ammonium (NH_4), dissolved iron (D-Fe, <0.22-μm), total dissolvable iron (T-Fe, unfiltered) and Chl-*a*. At selected times, water samples were collected for culture experiments and BSi determinations (Table 1). Seawater samples were collected from 5–300 m at one station (42°00′N, 145°15′E) using a set of 12 acid-cleaned, Teflon-coated, Niskin X 10-L sampling bottles (General Oceanic) attached to a carousel frame equipped with a Sea-Bird SBE-9 plus CTD sensor. Hydrographic conditions (temperature, salinity, sigma-*t* and dissolved oxygen) were obtained from CTD data.

2.2 Sample treatment and measurement

Samples for iron analysis were buffered at pH 3.2 with 10 mol L^{-1} quartz-distilled formic acid, 2.4 mol L^{-1} ammonium formate buffer solution and then kept at least 3 months for D-Fe, and 6 months for T-Fe at room temperature until analysis in a land laboratory. The iron concentration in each buffered sample was measured by an automated Fe analyzer (Kimoto Electric) using a combination of chelating resin concentration and luminol-hydrogen peroxide chemiluminescence detection in a closed flow-through system (Obata et al., 1993; Nakayama et al., this issue). The samples for macronutrient concentrations in seawater were frozen until a laboratory analysis and determined by a QuAAtro® continuous flow analyzer (Bran+Luebbe).

For Chl-*a* analysis, 100–300-mL of water samples were filtered on Whatman GF/F filter with gentle vacuum pressure (<100 mmHg). The Chl-*a* concentrations were measured by a Tuner Designs fluorometer (10-AU) according to the method of Welschmeyer (1994) after extraction by *N*, *N*-dimethylformamide (Suzuki and Ishimaru, 1990).

For BSi analysis, 1-L seawater was filtered through an 0.45-µm omnipore filter (Millipore) using an all-plastic filtration unit followed by rinsing with Milli-Q water (Millipore, >18.0 MΩ cm^{-1}). The filters were frozen in acrylic tubes at –20°C until analysis. The BSi was digested by heating the filters to 85°C for 2-hours in an 0.5% Na_2CO_3 solution (Merk, suprapur) to dissolve BSi (Paasche, 1980). After cooling, the solution was neutralized with 0.5 mol L^{-1} HCl. An aliquot of the solution was diluted with Milli-Q water, and analyzed by a QuAAtro® continuous flow analyzer. Data were corrected by subtracting an appropriate filter blank. Paasche's method (1980) should give less than 0.5% recovery of lithogenic mineral silica (Michel et al., 2002). The variability of the mean in duplicate BSi sample analyses was 2% in the present study.

2.3 Culture experiment

Three culture experiments were conducted on 9-March, 6- and 20-April 2007 (Table 1). Seawater for cultivation was collected at 10 m depth then sieved through 100-µm, acid-cleaned Teflon-mesh to eliminate mesozooplankton. The 100-µm mesh was sometimes

shaken gently to flush out chin-forming diatoms, after which there was no visible phytoplankton on the mesh. The seawater was then homogenized in an acid-washed 20-L polyethylene tank and dispensed into acid-cleaned 250-mL polycarbonate bottles (Nalgene) in a clean room on board. Incubation was at 5°C under 150-μmol photons m^{-2} s^{-1} of fluorescent light (12-h light:12-h dark). The macronutrients and Chl-*a* concentrations were measured initially and after 1-, 3- and 5-d incubations by the methods described above. The cultivation experiments were conducted in triplicate, nine bottles per experiment; bottles were sacrificed at each interval. Culture bottles were gently stirred by hand at least twice a day. Observation of the phytoplankton community initially and after 5-d of incubation was only done for the 6- and 20-April experiments using phase-contrast inverted microscopy following the method of Hasle (1978). An adequate volume of formalin-fixed sample was poured into the settling chamber (Hydro-bios), and settled for at least 24-h before identifications were made.

2.4 Data analysis

Macronutrient concentrations during winter were estimated by subtracting remineralized macronutrient concentrations from that below the MLD, which was estimated from the relationship between apparent oxygen utilization (AOU) and canonical Redfield ratio as reported previously (Tsurushima et al., 2002):

$$[\mathrm{Nut}]_{\mathrm{winter}} = [\mathrm{Nut}]_{in\ situ} - (\mathrm{AOU} \times \mathrm{Redfield\ ratio} \div 170) \quad (1)$$

where $[\mathrm{Nut}]_{\mathrm{winter}}$ and $[\mathrm{Nut}]_{in\ situ}$ represent for any macronutrient concentration during winter and that observed *in situ*, respectively. The Redfield ratios we used for macronutrient remineralization by heterotrophic activities were O_2:N:P = 170:16:1, reported by Anderson and Sarmiento (1994). In addition, we used O_2:Si = 170:15 to estimate [Si] during winter. However, Si remineralization does not occur solely by biological degradation processes, but mainly by thermodynamic dissolution (Dugdale and Wilkerson, 1998). The BSi dissolution rate is generally slower than those of particulate N or P, creating a downward "silica pump" (Dugdale and Wilkerson, 1998), and hence the deep [Si] maximum in the north Pacific Ocean is observed at least 1.5 times deeper (>1500 m) than those of N and P (~1000 m). In addition, Michel et al. (2002) reported based on linear regression analysis of BSi vs. particulate organic nitrogen (PON) that BSi flux is approximately 3 times higher than that of PON through the

150 m stratum during spring blooms. However, a conflicting observation was reported (Bidle et al., 2002, 2003) that the effect of a preferential remineralization of N and P compared to Si is diminished by bacterial attack. Thus the uncertainties affecting macronutrient remineralization ratios, especially for Si, have not yet been clarified (e.g., Dugdale and Wilkerson, 1998; Michel et al., 2002; Bidle et al., 2002, 2003). In addition, the amount of oxygen utilization other than by bacteria could be overestimated for purposes of estimating $[Nut]_{winter}$ in a relatively shallow and heterotrophic biomass-rich water column like that observed in the present study. During the spring bloom period in the Oyashio region, Shinada et al. (2001) reported that bacterial and microzooplankton production was approximately 67% of the secondary production. That indicates that normalized values of AOU could be overestimated by two-thirds, i.e., estimated $[Nut]_{winter}$ values could be underestimated and the gap amount may be transferred to higher trophic levels.

In the present study, the pycnocline during the April–May cruise was defined as the first downward increase in sigma-*t* of ≥ 0.02 m^{-1} and/or more than 2 weaker increases of $0.01 < \text{sigma-}t < 0.02$ m^{-1} in a 5 m stratum. In March, the pycnocline depth was defined as the inflection point of the vertical profile of sigma-*t* because the pycnocline was often very weak.

3. Results

*3.1 Physical properties and chlorophyll-*a *concentration*

During the OECOS cruises, seawater properties varied from cast to cast; however, all of the hydrography was within the previously observed ranges of the Oyashio current system (Hanawa and Mitsudera, 1987; Kono and Sato, this issue) (Fig. 1). In addition, the waters seemed to change by horizontal advection without respect to storm events at the station (Kono and Sato, this issue). In March, the waters were vertically homogenous down to 145 or 190 m with high temperature (5–6°C) and salinity (33.55–33.65). Then colder (~1°C) and warmer (~6°C) waters alternated in the upper 50 m during April to May, with coincident changes of salinity and sigma-*t* (Fig. 1a, b, c). Relatively warm, saline intrusions were observed in the 50 to 100 m stratum on 10-April and 18-April. Thus, the pycnocline depth depended on the water exchanges, but not on the thermocline or halocline alone; i.e. temperature and salinity were

211 little changed by local environmental forcing, and the water properties were conserved during
212 the present study (Fig. 1a, b, c; see also Kono and Sato, this issue). Chl-*a* in the surface mixed
213 layer during March to May observation periods varied approximately 2 orders of magnitude,
214 ranging from 0.38 μg L^{-1} on 6-March to 17.4 μg L^{-1} at 5m on 7-April (Fig. 1d). The higher
215 Chl-*a* concentrations occurred in the cold water system (<4°C) and *vice versa* (discussed
216 below).

217 The pycnocline below the surface mixed layer fluctuated from 8 to 129 m during the
218 April cruise (avg. 50.6 ± 33.5 m), extremes observed on 7-April and 16-April, respectively. In
219 March, the average was 170 m. Therefore, the present study describes the data from the upper
220 150 m, which we treat as an approximate seasonal maximum MLD in the Oyashio region.
221 However, the MLD in the Oyashio region during winter does fluctuate from year to year
222 (Harrison et al., 2004), varying in both location and timing of vertical shifts. The relationship
223 between physical properties and macronutrients was different below 150 m (see below).

224

225 *3.2 Nutrient and iron dynamics in spring*

226 Macronutrient concentrations below the MLD were less at higher temperatures.
227 Ranges were 11.3–27.5 μmol L^{-1} for N+N, 1.25–2.46 μmol L^{-1} for P, and 15.1–59.1 μmol L^{-1}
228 for Si (Fig. 2). The relationships of nutrients with salinity below the MLD were weaker than
229 those with temperature (data not shown), possibly because salinity-nutrient ratios differ
230 between cold oceanic Oyashio and cold coastal Oyashio waters (these water types are
231 described by Kono and Sato, this issue). The relationships among temperature and
232 macronutrients are different below 200 m from those in the upper 150 m. That is,
233 macronutrient concentrations increased with increase in temperature (data not shown). A deep
234 temperature maximum (>200 m) is one of the characteristics of the Oyashio region during
235 winter and into spring (e.g. Kono, 1997). In the upper mixed layer, N+N, P, and Si ranges
236 were 1.88–18.8, 0.64–1.85, and 3.14–35.7 μmol L^{-1}, respectively (Fig. 2), concentrations
237 significantly lower compared to those below the MLD ($p<0.001$, ANOVA).

238 The molar ratio of (N+N):P was always less than the Redfield ratio of 16 (Redfield et
239 al., 1963), ranging from 2.8 to 11.4. The lowest values were observed in the colder waters
240 (Fig. 3a). The Si:P ratio was highly variable in the upper mixed layer, 4.4 to 22.8 whereas

below the MLD the range was 13.0 to 24.1 (Fig. 3b). Below the MLD, Si:(N+N) slightly decreased as temperature increased; it was greater than the Redfield ratio (Redfield et al., 1963; Brzezinski, 1985) even in the warmer waters. The Si:(N+N) ratio varied in the upper mixed layer from 0.55 to 3.39 with the high ratios in the colder waters and *vice versa* (Fig. 3c). The (N+N):P:Si ratio in March observations was close to constant at 10.9 ± 0.4:1:19.6 ± 1.1 (mean ratio to P ± 1 SD), whereas 1 SD of the Si:(N+N) ratio was 0.07. Thus, wide variations of nutrient stoichiometry were observed only in the 6-April to 1-May period, which was also the case for Chl-*a* variation. The concentrations of T-Fe and D-Fe also seemed to decrease with increase in temperature, with significantly higher T-Fe and D-Fe concentrations below the MLD than near the surface ($p<0.001$, ANOVA). In the water above ~4°C, T-Fe was lower than 5.5 nmol L^{-1}, while in colder waters T-Fe concentrations were sometimes above 10 nmol L^{-1} (Fig. 4b, see also Nakayama et al., this issue).

The NH_4 concentration was <0.2 μmol L^{-1} in the upper 50 m stratum and <0.1 μmol L^{-1} below 75 m during the pre-bloom period in March (Fig. 5a). In general, a subsurface NH_4 maximum with values from 0.5–1.3 μmol L^{-1} was observed during April–early May below the surface layer with high chlorophyll (Fig. 5b). However, 5 out of 19 hydro-casts (10-, 13-, 24-, 25- and 26-April) when the different water mass intrusions into the subsurface (20–100 m) were observed (Fig. 1), a relatively broad zone of high subsurface NH_4 (>1 μmol L^{-1} maximum) occurred within the upper mixed layer (Fig. 5c). There was no consistent relationship between NH_4 and physical or other chemical properties.

3.3 Biogenic silica

The BSi concentration increased with Chl-*a* concentration (Fig. 6a). During pre-bloom period, the BSi and Chl-*a* concentrations were approximately constant at ~0.45 μmol L^{-1} and ~0.4 μg L^{-1}, respectively (insert in Fig. 6a). The BSi concentration at 5 m ranged from 1.4 (17-April) to 16.7 μmol L^{-1} (6-April) during the bloom. About a half of measured BSi concentration measurements taken below the MLD during the bloom were higher than those during the pre-bloom period. In the upper mixed layer, the regression slope between BSi and Chl-*a* concentration was significantly higher in the warmer (>4°C) water than in the colder (<4°C) water (*F*-test; Fig. 6b).

3.4 Culture experiment

We conducted one culture experiment during colder conditions with high D-Fe and T-Fe, and two experiments during warmer conditions with low T-Fe (Table 2). The initial phytoplankton communities in March were dominated by pico- and nano-eukaryotic phytoplankton taxa such as Parmophyceae (2–5 μm) (Ichinomiya et al., this issue). On 6 April, large chain-forming diatoms (Bacillariophyceae) (>20 μm) predominated: *Thalassiosira nordenskioeldii* (abundance contribution: 22.6%), other *Thalassiosira* spp. (33.5%), and *Chaetoceros* subgenus *Hyalochaete* (38.0%), followed by *Odontella aurita* (2.1%) and *Porosira* sp. cf. *pentaportula* (1.4%). On 20-April, the numerically dominant diatom species was *Chaetoceros* subgenus *Hyalochaete* (78.0%), followed by *T. nordenskioeldii* (4.1%), *T. anguste-lineata* (4.0%), other *Thalassiosira* spp. (8.5%), *Fragilariopsis* sp. cf. *oceanica* (1.4%) and *Neodenticula seminae* (1.3%) (see also Sato and Furuya, this issue, for dynamics of small phytoplankton). The un-screened natural diatom community examined by SEM (Hattori-Saito, et al., unpublished data), had similar generic composition to that observed in the present study. It is notable that the temperate-zone diatom *Asteromphalus flabellatus* (Kawarada et al., 1968; Hasle and Syvertsen, 1997) was detected in the 20-April community but not in that of 6-April. In addition, approximately 6% of the diatoms such as *Chaetoceros* subgenus *Hyalochaete* and *Stephanopyxis nipponica* formed resting spores at the start of the 20-April culture experiment (Sugie et al., in press).

The Chl-*a* growth rate during the 6-April cultivation was 0.55 d^{-1} during the first day. Due to both N- and Si-depletion after 3 d of cultivation, Chl-*a* biomass reached stationary phase (Fig. 7a, b, d). In the March and 20-April incubations, Chl-*a* biomass increased exponentially throughout the 5-d cultivation periods with Chl-*a*-specific growth rates of 0.29 and 0.14 d^{-1}, respectively (Fig. 7a). In the 20-April cultivation, Si was exhausted after 5 d without N- or P-depletion. The non-siliceous flagellate *Phaeocystis globosa* and/or *P. pouchetii* (Prymnesiophyceae) increased, which may have contributed to Chl-*a* increase in days 3 to 5 of cultivation. Phosphate remained more than 0.2 μmol L^{-1} at the end of the experiment in all cultivations (Fig. 7c). Ammonia concentrations did not vary during the cultivation period of March, whereas both April cultivations exhausted ammonia at 5 d as

well as N+N (data not shown). The nutrient utilization rate per unit Chl-*a* during culture growth was calculated from the initial level to that before any nutrient exhaustion, i.e. the initial 5 d for the March incubation, initial 1 d for 6-April, and initial 3 d for 20-April (Fig. 7). The ΔNut / ΔChl-*a* ratios differed among experiments, which may have derived from the differences in the phytoplankton communities and iron concentrations (Table 2).

3.4 Macronutrients below the MLD

The AOU below the MLD ranged from 11.1 to 113.5 μmol L^{-1}, except for one negative AOU at 30 m depth on 8-April when the MLD was 21 m. This indicates N+N, P and Si remineralization amounting to 1.0–10.7, 0.07–0.67 and 0.9–10.0 μmol L^{-1}, respectively, in the 150 m stratum (excluding the one negative AOU datum). The remineralized macronutrient concentrations indicate that 5.9–39% of the N+N, 3.6–28% of P, and 2.6–18% of Si were already regenerated during the bloom periods. The lower amounts of remineralized macronutrients were generally observed in the colder, high-Chl-*a* waters. The $[Nut]_{winter}$ values were negatively correlated with an increased contribution of warm, saline Modified Kuroshio Water (MKW) (Fig. 8 a, b, c; and see the water mass mixing ratio described by Kono and Sato, this issue). However, as stated earlier, respiration of organisms other than bacteria and microzooplankton was ignored in the present estimates, and they may contribute up to a third of the community respiration (Shinada et al., 2001). This missing third (approximately) implies that the estimated macronutrient remineralizations potentially were 8.7–58% of N+N, 5.3–41% of P, and 3.8–26% of Si. However, the correlation coefficient decreased from 0.70 to 0.17 for N+N, 0.77 to 0.31 for P, and 0.53 to 0.35 for Si by taking into account respiration other than that of bacteria and microzooplankton (data not shown). Even with such uncertainty, the macronutrient concentrations during winter estimated by equation (1), decreased significantly when there was an increased contribution of MKW (Fig. 8a, b and c). The $[N+N]_{winter}$:$[P]_{winter}$ ratio slightly decreased from ~10 to 8.7 (mol:mol) during increased contribution of the MKW (Fig. 8d). The $[Si]_{winter}$:$[P]_{winter}$ and $[Si]_{winter}$:$[N+N]_{winter}$ significantly decreased (*F*-test, $p<0.001$) with increased MKW contribution (Fig. 8d).

4. Discussion

331

332 During the OECOS-West study at Stn. A5, the variations of macronutrients and iron
333 concentrations covered the entire range observed from winter to summer in the Oyashio
334 region (Kasai et al., 2001; Nishioka et al., 2007). Those large variations derived from variable
335 amounts of biological utilization (Figs. 1, 2, 4, 5 and 6) and variable nutrient supply due to
336 recurring water mass exchanges (Figs. 2, 3 and 8). The spring phytoplankton bloom
337 progression and the chemical and hydrographical conditions did not seem to be strictly
338 time-dependent changes (Fig. 1). That is, seasonality was a minor component of the
339 characteristics for each bloom patch in the present study. In addition, nutritional status
340 especially iron availability for phytoplankton, was different among the bloom patches during
341 spring in the Oyashio region (Figs. 6 and 7). Relatively large amounts of macronutrients were
342 already remineralized in the upper 150 m stratum; however, the remineralized nutrient
343 concentrations also varied by an order of magnitude (Figs. 5 and 8). That variability had never
344 been detected before due to low-frequency sampling.

345

346 *4.1 Nutritional status of the spring phytoplankton community*

347 The siliceous phytoplankton community was quite different between the March and
348 April experiments. In March there were Parmophyceae (Ichinomiya et al., this issue), while in
349 April there were predominantly large chain-forming diatoms, as reported previously during
350 spring in the western subarctic Pacific (Saito and Tsuda, 2003; Liu et al., 2004). The nutrient
351 drawdown ratios of the March cultivation experiment may have derived from pico- and
352 nano-phytoplankton; however, their nutritional status could not be discerned further. That is
353 because one of the dominant siliceous phytoplankters belonged to the Parmophyceae
354 (Heterokontophyta, Chrysophytes: Booth and Marchant, 1987). Parmophyceae have spherical
355 or quasi-spherical siliceous skeleton surrounding a cell approximately 2–5 μm in size. They
356 are sometimes the dominant phytoplankton during non-bloom periods in the North Pacific
357 regions (Booth et al., 1980; Taniguchi et al., 1995; Komuro et al., 2005) and the Southern
358 Ocean (Silver et al., 1980). However, they have not been cultured, and belong to taxa for
359 which little information is available (Ichinomiya et al., this issue).

360 The phytoplankton cultivated from the 6-April community, were predominantly

centric diatoms growing in nearly optimum conditions with a nearly optimum Si:N drawdown ratio of 0.73 ± 0.07 (Saito and Tsuda, 2003); hence there was a high Chl-*a* specific growth rate of 0.55 d^{-1}, comparable to the optimal rates of *T. nordenskioeldii* in unialgal culture at 5°C. That was the strain isolated during this cruise (Sugie and Kuma, 2008) and one of the dominant species in the incubation bottle. On the other hand, in the 20-April experiment, relatively ample macronutrient but low D-Fe concentrations (<0.2 nmol L^{-1}) possibly made phytoplankton community growth rate slow (0.14 d^{-1}: the initial 3 days) with nearly double Si:N drawdown ratio (1.22 ± 0.06) compared to the 6-April experiments. However, two dominant diatom genera such as *Thalassiosira* spp. and *Chaetoceros* subgenus *Hyalochaete* spp. were conservative in both experiments. Thus, the higher Si:N drawdown ratio of the 20-April community was associated with heavily silicified and/or N-quota reduced iron-limited diatoms (Takeda, 1998; Marchetti and Harrison, 2007) and diatom resting spores under either N- or Fe-limited conditions (Sugie and Kuma, 2008; Sugie et al., in press). Because the diatom resting spores have several-fold higher Si quota than N quota (e.g. Kuwata et al., 1993), even if resting spores were only 6% of the total diatom community, that would significantly increase the Si drawdown (Sugie et al., in press). In addition, iron-limited diatoms reduce their Chl-*a* cell quota, increase their C:Chl-*a* ratio and maintain relatively constant C:N ratio (Price, 2005). Thus, Chl-*a*-specific nutrient drawdown rates (Table 2) possibly increased due to iron-limitation of the phytoplankton community in the 20-April cultivation.

The BSi to Chl-*a* ratio also increased significantly in the warmer water mass and decreased in the colder waters (Fig. 6). In the *in situ* phytoplankton community analysis, the Chl-*a* content of the >10 μm fraction was at least 80% of the total, and diatoms were predominant in the community throughout the bloom period (Isada et al., this issue; Hattori-Saito A., unpublished data). Approximately 2-fold higher BSi to Chl-*a* ratio in the warm water than cold water was due to the physiological response of diatoms affected by iron- and/or light-limited conditions. However, the MLD was deeper in the warm water system than in the cold water system (Fig. 9). Light-limited phytoplankton have high intracellular Chl-*a* concentration (Thompson et al., 1989), and so likely, the increase in BSi to Chl-*a* ratio in the warm water represents an increase in Si quota of the diatoms caused mainly

391 by iron-limitation. Therefore, the iron status of the phytoplankton community in the spring
392 bloom may vary from iron-replete to iron-limited in colder and warmer waters, respectively
393 (Figs. 6 and 7, Table 2).
394
395 *4.2 The MLD and spring bloom*
396 The pycnocline (sigma t = 26.49 ± 0.05, avg. ± 1SD) was generally coincident with
397 the layer in which Chl-*a* decreased to <1 μg Chl-*a* L^{-1}; this 'chlorocline' was usually in the
398 layer between 26.5 and 26.6 sigma-*t* (avg. 26.52 ± 0.04; Fig. 1c, d). The MLD and
399 temperature had significantly negative correlations with surface-layer (5 m) Chl-*a* (Fig. 9a, b),
400 while T-Fe correlated positively with surface Chl-*a* (Fig. 9c). The correlation was weaker for
401 Chl-*a* vs. *in situ* macronutrient concentrations (shown only for N+N, Fig. 9d). In addition,
402 there was no relationship of Chl-*a* with D-Fe (Fig. 9e), which implies variable phytoplankton
403 utilization and growth under different macro- and micronutrient environments. Apparently
404 surface Chl-*a* was controlled by light availability and physical dilution of phytoplankton
405 biomass in the mixed layer, as reported previously for the Oyashio region (Saito et al., 2002)
406 and for mesoscale *in situ* iron-fertilization experiments (de Baar et al., 2005). That is, in the
407 present study, the cold water mass with shallower MLD had higher Chl-*a* concentration, while
408 the warmer water mass with deeper MLD had lower Chl-*a* (Fig. 9a, f). In general, the
409 initiation and development of a spring phytoplankton bloom is a seasonal phenomenon driven
410 by increase in irradiance and day-length, and by shoaling of the MLD during the transition
411 from winter to spring (Smetacek and Passow, 1990). Initiation and seasonal timing of the
412 spring bloom in the Oyashio region have been investigated by a combination of satellite
413 imagery and Argo float data, described elsewhere (Okamoto et al., this issue). However, in the
414 present study, the variation of the water column conditions generated a mosaic of bloom
415 patches rather than a simple seasonal succession driven by progressive thermal stratification
416 (Figs. 1 and 9).
417
418 *4.3 Nutrients and spring bloom dynamics in the western subarctic Pacific Ocean*
419 *4.3.1 Colder water system*
420 Below the MLD of the Oyashio region, there is a tendency for decreasing

421 macronutrient concentrations with increasing in temperature (Fig. 2), as previously observed
422 in the Western Subarctic Gyre (Andreev et al., 2002). In addition, Si decreases preferentially
423 with increasing temperature compared to N and P (Fig. 3), which could be caused by greater
424 contributions of MKW (Fig. 8). Variable macronutrient utilization by phytoplankton with
425 different nutritional status may also change the relative macronutrient concentrations (Fig. 2).
426 A substantial macronutrient drawdown occurred during the spring bloom period (Fig. 2), and
427 surprisingly, relatively great macronutrient remineralization occurred at the same time in the
428 upper 150 m stratum, as supported by our ammonium data (Fig. 5).
429 The (N+N):P:Si ratio below the MLD and the ratio during the March pre-bloom
430 period in the Oyashio region indicate that the exhaustion of nitrogenous nutrient would
431 terminate the spring phytoplankton bloom in the region within the temperature range observed
432 in the present study (Figs. 3 and 8), provided that phytoplankton utilize macronutrients at the
433 Redfield ratio (Redfield et al., 1963; Brzezinski, 1985). The residual Si:(N+N) would increase
434 with the bloom progression, if the diatoms utilize macronutrients at the Redfield ratio and/or
435 if non-diatom species increased. The increase would persist until just before N exhaustion. In
436 the iron-rich subarctic water of Funka Bay, Japan where the pre-bloom periods of *in situ* Si:N
437 ratio is ~2, the spring phytoplankton bloom is terminated by nitrate depletion (Kudo et al.,
438 2000; Kuma et al., 2000). The Si:N ratio increased because the Si:N drawdown ratio of a
439 predominantly diatom community is <1 before nitrate depletion (Kudo et al., 2000). In the
440 present study, in the 6- to 8-April period under cold and iron-replete conditions, the Si:(N+N)
441 ratio in the upper mixed layer increased to a maximum of ~3.4 with the progress of the diatom
442 bloom (Fig. 3c). In addition, the dominant diatom species are reported to form heavily
443 silicified resting spores under N-deplete conditions (McQuoid and Hobson, 1996; Sugie et al.,
444 in press). These diatoms would exhaust Si soon after N-depletion by formation of resting
445 spores in the colder water system, as suggested for Funka Bay (Kudo et al., 2000) and for the
446 Oyashio region (Saito and Tsuda, 2003). Unfortunately, in our culture experiment of 6-April,
447 the contribution of resting spores to the diatom community was <1%, probably due to the
448 short cultivation time after N-exhaustion or to inhibition of further silicification of the spore
449 frustules by Si-depletion (Fig. 7). Therefore, the bloom in the colder, iron- and nutrient-rich
450 water with shallower MLD (Figs. 1, 8 and 9) develops rapidly and achieves quite high

biomass. Thereafter, the bloom is terminated by nitrogenous nutrient exhaustion.

The bloom duration (n-days) in the cold (1°C), iron-rich, eventually N-limited water can be calculated as follows:

$$[\mathrm{Nut}]_{\mathrm{winter}} - \left(\sum_{t=0}^{n} [\text{Chl-}a]_{\mathrm{winter}} \times e^{\mu \times t}\right) \times \Delta[\mathrm{Nut}]/\Delta[\text{Chl-}a] = 0, \qquad (2)$$

we took the initial Chl-*a* (day 0) to be approximately the March value of 0.4 μg L^{-1} (Fig. 1d), the growth rates (μ) to be 0.55 d^{-1} (Fig. 5a), and ΔN / ΔChl-*a* to be 1.32 (Table 2). The quantity $[\mathrm{Nut}]_{\mathrm{winter}}$ represents estimated macronutrient concentration during winter of the element limiting the carrying capacity. We took the maximum nutrient concentration to be approximately that below the MLD without any admixture of MKW, that is 18.7 μmol L^{-1} for $[\mathrm{N+N}]_{\mathrm{winter}}$ (Fig. 8a). Then, the calculated duration is only 6–7 days, and maximum [Chl-*a*] would be ca. 14 μg L^{-1}, similar to the [Chl-*a*] in the nearly N-depleted (~2 μmol L^{-1}), iron-rich (T-Fe ≈ 20 nmol L^{-1}), and colder water (~2°C) bloom condition (Chl-*a*: 17 μmol L^{-1}) of 7-April at 5 m (Fig. 1).

The calculated duration would change if mesozooplankton grazing could be taken into account. Nevertheless, mesozooplankton grazing is thought to be low because mesozooplankton metabolism is depressed by cold water temperature during the bloom period (Ikeda, 1985; Rose and Caron, 2007; Kobari et al., this issue a). In fact, short-term massive blooms have been observed to sink to depth without significant mesozooplankton grazing in the other regions characterized by near-zero water temperatures (Michel et al., 2002; Thompson et al., 2008). The high biomass at N-limitation may enhance formation of fast-sinking aggregates, including heavy resting spores (Sugie and Kuma, 2008), accelerating the bloom collapse by sedimentation (Grimm et al., 1997; Kudo et al., 2000; Kristiansen et al., 2001; Michel et al., 2002). Unfortunately, we could not detect the bloom-collapse, at least partly due to the recurring shifts of the water mass at the sampling station. We should try in future work to determine the fate of the bloom in the Oyashio region.

4.3.2 Warmer water system

Silicic acid decreased preferentially compared to the other macronutrients in the warmer water mass (Figs. 2, 3 and 8). Although there was higher $[\mathrm{Si}]_{\mathrm{winter}}$ compared to

480 $[N+N]_{winter}$ in the warm water (Fig. 8), the iron-limited heavily silicified diatoms (Takeda,
481 1998; Marchetti and Harrison, 2007) and diatom resting spores (Kuwata et al., 1993; Sugie
482 and Kuma, 2008; Sugie et al., in press) would have decreased the *in situ* Si:(N+N) ratio to <1
483 with progress the bloom (Fig. 3c). In the present study, lower D-Fe concentration (<0.2 μmol
484 L^{-1}) compared to previously measured values in the western subarctic Pacific region
485 (Nishioka et al., 2003, 2007; Takata et al., 2006) was observed in the warmer water (>3–4°C).
486 Saito et al. (2002) also reported that two-thirds of the Oyashio waters at 20–30 m depth in
487 August retained relatively abundant macronutrients, similarly to HNLC conditions. The D-Fe
488 and T-Fe seem to decrease with increase in temperature, similarly to macronutrients (Figs. 2
489 and 4), and the 20-April incubation indicated that the *in situ* diatom community was
490 iron-limited in even mildly warmer waters (Fig. 7, Table 2). Additionally, the warm water
491 generally had a deep MLD (Fig. 9e) and chlorocline (>50 m, Fig. 1d), often deeper than the
492 level of 1% of photosynthetically active radiation at the surface (Isada et al., this issue).
493 Therefore, the development of a bloom in the warmer waters would be affected by iron- and
494 light-colimitation and by dilution of the phytoplankton biomass in the deep mixed layer.
495 The relationship between $[Si]_{winter}$ and temperature has a lower correlation coefficient
496 than those of $[N]_{winter}$ and $[P]_{winter}$, possibly associated with the variability of the BSi
497 dissolution kinetics in the water column (Michel et al., 2002; Bidle et al., 2002, 2003). In
498 addition, the variability of diatom silicification, due to their nutritional status in the upper
499 mixed layer, could change the remineralization stoichiometry below the mixed layer.
500 However in the present estimation, we used remineralization stoichiometry at constant
501 Redfield ratios (Redfield et al., 1963; Brzezinski, 1985). Another possibility may involve the
502 difference of the $[Si]_{winter}$ value between Coastal Oyashio Water and Oyashio Water, however,
503 we could not characterize that from our data. Although silicon dynamics have these
504 uncertainties, a decrease in $[Si]_{winter}$ with temperature is a significantly conservative trend.
505 Our results indicate that diatom production in the warmer water with relatively deep
506 MLD was reduced not only by lesser amounts of Si but possibly also by formation of heavily
507 silicified diatom vegetative cells and resting spores under iron-limitation (Takeda, 1998;
508 Marchetti and Harrison, 2007; Sugie and Kuma, 2008; Sugie et al., in press), combined with
509 further silicification due to light-limitation (Saito and Tsuda, 2003). However, the specific

factors limiting diatom production (de Baar, 1994) could not be assessed from stoichiometry. There is a much higher concentration of particulate iron in the Oyashio region compared to the eastern subarctic Pacific region (Nishioka et al., 2003; Takata et al., 2006; Nakayama et a., this issue), which could release bioavailable D-Fe. On the other hand, the [D-Fe] could be decreased by particle scavenging. However, the amount of D-Fe released from particulate iron or scavenged is unknown. In addition, relatively high ammonium concentration in the mixed layer (Fig. 5) may decrease nitrate uptake (Dortch et al., 1991), which would enhance Si utilization compared to N+N and/or lead to N+N remaining utilized, as observed for HNLC-like conditions in the Oyashio region (Saito et al., 2002). The present study partly illustrates that the warmer water type could be significantly linked to HNLC-like conditions in subsurface layer of the Oyashio region (Saito et al., 2002).

Another interest of the warmer water type is the bloom duration and favorable food environment for herbivorous zooplankton. The bloom duration in water with the highest MKW contribution water (~0.65) can be calculated from equation (2). The bloom duration in the iron- and Si-limited ($[Si]_{winter} \approx 19$ μmol L^{-1}) water lasted ~19 days, using 0.14 d^{-1} as the growth rate (Fig. 5a), and ΔSi / ΔChl-*a* of 3.29 (Table 2). From the viewpoint of trophodynamics, warm water accelerates overall metabolism of herbivorous heterotrophs including their grazing activities (Ikeda, 1985; Rose and Caron, 2007; Kobari et al., this issue a). Significant implications of the increased grazing activity of herbivorous heterotrophs are (1) to improve transfer efficiency between phytoplankton and higher trophic levels, and (2) to act as one of significant factors terminating the bloom (Takahashi et al., 2008; Kobari et al., this issue b), especially after the phytoplankton growth is limited by iron- and/or Si-limitation.

The present study indicated that (1) the physical water properties during winter in the Oyashio region determined nutrient and iron concentrations in the water mass, (2) iron and MLD regulate the development rate, and (3) these same factors probably control the fate of the spring diatom bloom. We found that the carrying capacity of the Oyashio region for phytoplankton in the spring bloom period is a spatial and advective mosaic. The annual new production may vary a great deal due to the differences between the water masses present at a given time or site in the Oyashio region. These bloom dynamics would affect the biological pump and the transfer efficiency to higher trophic levels, although such frequent variability

also seemingly supports high productivity in the Oyashio region.

Acknowledgments

We thank the captain, crews and colleagues aboard the TS Oshoro-Maru and RV Hakuho-Maru for their efforts at sea. We are grateful to Dr. Kono T. in the Tokai University for providing the water mass mixing-ratio analysis. We would like to thank Dr. Ichinomiya M. in the Tohoku National Fisheries Research Institute, Dr. Gomi Y. in the Seikai National Fisheries Research Institute, Dr. Kobari T in the Kagoshima University, Dr. Ota T. in the Ishinomaki Sensyu University, Dr. Sato M. in the University of Tokyo, and Dr. Suzuki K. and Ms. Omata A. in the Hokkaido University for their technical support for microscopic observations and useful discussions. We also thank Mr. Isada T. and Ms. Hattori-Saito A. in the Hokkaido University for supporting our sampling. We acknowledge three anonymous reviewers for valuable comments. This work was supported by grants for Scientific Research (18201001) from the Ministry of Education, Culture, Sports, Science and Technology and for the Sasakawa Scientific Research Grant from the Japan Science Society.

References

Anderson, L.A., Sarmiento, J. L., 1994. Redfield ratios of remineralization determined by nutrient data analysis. Global Biogeochemical Cycles 8, 65–80.

Andreev, A., Kusakabe, M., Honda, M., Murata, A., Saito, C., 2002. Vertical fluxes of nutrients and carbon through the halocline in the western subarctic Gyre calculated by mass balance. Deep-Sea Research II 49, 5577–5593.

Banse, K., English, D.C., 1999. Comparing phytoplankton seasonality in the eastern and western subarctic Pacific and the western Bering Sea. Progress in Oceanography 43, 235–288.

Bidle, K.D., Manganelli, M., Azam, F., 2002. Regulation of oceanic silicon and carbon preservation by temperature control on bacteria. Science 298, 1980–1984.

Bidle, K. D., Brzezinski, M. A., Long, R. A., Jones, J. L., Azam, F., 2003. Diminished

efficiency in the oceanic silica pump caused by bacteria mediated silica dissolution. Limnology and Oceanography 48, 1855–1868.

Booth, B.C., Lewin, J., Norris, R.E., 1980. Siliceous nanoplankton I. Newly discovered cysts from the Gulf of Alaska. Marine Biology 58, 205–209.

Booth, B.C., Marchant, H.J., 1987. Parmales, a new order of marine chrysophytes, with descriptions of three new genera and seven new species. Journal of Phycology 23, 245-260

Boyd, P.W., Law, C.S., Wong, C.S., Nojiri, Y., Tsuda, A., Levasseur, M., Takeda, S., Rivkin, R., Harrison, P.J., Strzepek, R., Gower, J., McKay, R.M., Abraham, E., Arychuk, M., Barwell-Clarke, J., Crawford, W., Crawford, D., Hale, M., Harada, K., Johnson, K., Kiyosawa, H., Kudo, I., Marchetti, A., Miller, W., Needoba, J., Nishioka, J., Ogawa, H., Page, J., Robert, M., Saito, H., Sastri, A., Sherry, N., Soutar, T., Sutherland, N., Taira, Y., Whitney, F., Wong, S.K.E., Yoshimura, T., 2004. The decline and fate of an iron-induced subarctic phytoplankton bloom. Nature 428, 549–553.

Bruland, K.W., Rue, E.L., Smith, G.J., 2001. Iron and macronutrients in California coastal upwelling regimes: Implications for diatom bloom. Limnology and Oceanography 46, 1661–1674.

Bruland, K.W., Rue, E.L., Smith, G.J., DiTullio, G.R., 2005. Iron, macronutrients and diatom blooms in the Peru upwelling regime: brown and blue waters of Peru. Marine Chemistry 93, 81–103.

Brzezinski, M.A., 1985. The Si:C:N ratio of marine diatoms: interspecific variability and the effect of some environmental variables. Journal of Phycology 21, 347–357.

de Baar, H.J.W., 1994. von Liebig's Law of the Minimum and plankton ecology (1899–1991). Progress in Oceanography 33, 347–386.

de Baar, H.J.W., Boyd, P.W., Coale, K.H., Landry, M.R., Tsuda, A., Assmy, P., Bakker, D.C.E., Bozec, Y., Barber, R.T., Brzezinski, M.A., Buesseler, K.O., Boyé, M., Croot, P.L., Gervais, F., Gorbunov, Y., Harrison, P.J., Hiscock, W.T., Laan, P., Lancelot, C., Law, C.S., Levasseur, M., Marchetti, A., Millero, F.J., Nishioka, J., Nojiri, Y., van Oijen, T., Riebesell, U., Rijkenberg, M.J.A., Saito, H., Takeda, S., Timmermans, K.R., Veldhuis, M.J.W., Waite, A.M., Wong, C.S., 2005. Synthesis of iron fertilization experiments:

From the Iron Age in the Age of Enlightenment. Journal of Geophysical Research 110, C09S16, doi:10.1029/2004JC002601.

Dortch, Q., Thompson, P.A., Harrison, P.J., 1991. Short-term interaction between nitrate and ammonium uptake in *Thalassiosira pseudonana*: Effect of preconditioning nitrogen source and growth rate. Marine Biology 110, 183–193.

Dugdale, R.C., Wilkerson, F.P., 1998. Silicate regulation of new production in the equatorial Pacific upwelling. Nature 391, 270–273.

Grimm, K.A., Lange, C.B., Gill, A.S., 1997. Self-sedimentation of phytoplankton blooms in the geologic record. Sedimentary Geology 110, 151–161.

Hanawa, K., Mitsudera, H., 1987. Variation of water system distribution in the Sanriku coastal area. Journal of the Oceanographical Society of Japan 42, 435–446.

Harrison, P.J., Whitney, F.A., Tsuda, A., Saito, H., Tadokoro, K., 2004. Nutrient and plankton dynamics in the NE and NW gyres of the subarctic Pacific Ocean. Journal of Oceanography 60, 93–117.

Hasle, G.R., 1978. Using the inverted microscope. In: Sournia, A., (Ed.) Phytoplankton manual. UNESCO, Paris, pp 191–196.

Hasle, G.R., Syvertsen, E.E., 1997. Marine diatoms. In: Tomas CR (Ed.) Identifying Marine Phytoplankton. Academic Press, London, pp 5–385.

Hutchins, D.A., DiTullio, G., Zhang, Y., Bruland, K.W., 1998. An iron limitation mosaic in the California upwelling regime. Limnology and Oceanography 43, 1037–1054.

Ichinomiya, M., Gomi, Y., Nakamachi, M., Ota, T., Kobari, T., Temporal patterns in silica deposition among siliceous plankton during the spring bloom in the Oyashio region. Deep-Sea Research II, this issue.

Ikeda, T., 1985. Metabolic rates of epipelagic marine zooplankton as a function of body mass and temperature. Marine Biology 85, 1–11.

Isada, T., Hattori-Saito, A., Saito, H., Ikeda, T., Suzuki, K., Primary productivity in the Oyashio region of the northwest subarctic Pacific during the spring bloom as measured with ^{13}C technique and satellite remote sensing. Deep-Sea Research II, this issue.

Kasai, H., Saito, H., Kashiwai, M., Taneda, T., Kusaka, A., Kawasaki, Y., Kono, T., Taguchi, S., Tsuda, A., 2001. Seasonal and interannual variations in nutrients and plankton in the

630 Oyashio region: A summary of a 10-years observation along the *A-line*. Bulletin of
631 Hokkaido National Fisheries Research Institute 64, 55–134.
632 Kawarada, Y., Kitou, M., Furuhashi, K., Sano, A., 1968. Distribution of plankton in the waters
633 neighboring Japan in 1966 (CSK). The Oceanographical Magazine 20, 187–212.
634 Kobari, T., Ueda, A., Nishibe, Y., a. Development and growth of ontogenetically migrating
635 copepods during the spring phytoplankton bloom in the Oyashio region. Deep-Sea
636 Research II, this issue.
637 Kobari, T., Inoue, Y., Nakamura, Y., Okamura, H., Ota, T., Nishibe, Y., Ichinomiya, M., b.
638 Feeding impacts of ontogenetically migrating copepods on food webs during the spring
639 phytoplankton bloom in the Oyashio region. Deep-Sea Research II, this issue.
640 Komuro, C., Narita, H., Imai, K., Nojiri, Y., Jordan, R.W., 2005. Microplankton assemblages
641 at Station KNOT in the subarctic western Pacific, 1999–2000. Deep-Sea Research II 52,
642 2206–2217.
643 Kono, T., 1997. Modification of the Oyashio Water in the Hokkaido and Tohoku areas.
644 Deep-Sea Research I 44, 669–688.
645 Kono, T., Kawasaki, Y., 1997. Modification of the western subarctic water by exchange with
646 the Okhotsk Sea. Deep-Sea Research I 44, 689–711.
647 Kono, T., Sato, M., A mixing analysis of the surface water in the Oyashio region and its
648 application to the spring bloom dynamics. Deep-Sea Research II, this issue.
649 Kristiansen, S., Farbrot, T., Naustvoll, L.J., 2001. Spring bloom nutrient dynamics in the
650 Oslofjord. Marine Ecology Progress Series 219, 41–49.
651 Kudo, I., Yoshimura, T., Yanada, M., Matsunaga, K., 2000. Exhaustion of nitrate terminates a
652 phytoplankton bloom in Funka Bay, Japan: change in SiO_4:NO_3 consumption rate during
653 the bloom. Marine Ecology Progress Series 193, 45–51.
654 Kuma, K., Katsumoto, A., Shiga, N., Sawabe, T., Matsunaga, K., 2000. Variation of
655 size-fractionated Fe concentrations and Fe(III) hydroxide solubilities during a spring
656 phytoplankton bloom in Funka Bay (Japan). Marine Chemistry 71, 111–123.
657 Kuwata, A., Hama, T., Takahashi, M., 1993. Ecophysiological characterization of two life
658 forms, resting spores and resting cells, of a marine planktonic diatom, *Chaetoceros*
659 *pseudocurvisetus*, formed under nutrient depletion. Marine Ecology Progress Series 102,

245–255.

Liu, H., Suzuki, K., Saito, H., 2004. Community structure and dynamics of phytoplankton in the western subarctic Pacific Ocean: A synthesis. Journal of Oceanography 60, 119–137.

Marchetti, A., Harrison, P.J., 2007. Coupled changes in the cell morphology and the elemental (C, N, and Si) composition of the pennate diatom *Pseudo-nitzschia* due to iron deficiency. Limnology and Oceanography 52, 2270–2284.

McQuoid, M.R., Hobson, L.A., 1996. Diatom resting stages. Journal of Phycology 32, 889–902.

Michel, C., Gosselin, M., Nozais, C., 2002. Preferential sinking export of biogenic silica during the spring and summer in the North Water Polynya (northern Baffin Bay): Temperature or biological control? Journal of Geophysical Research 107, C7, 3064, doi:10.1029/2000JC000408.

Nakayama, Y., Kuma, K., Fujita, S., Sugie, K., Ikeda, T., Temporal variability and bioavailability of iron and nutrient during spring phytoplankton bloom in the Oyashio region. Deep-Sea Research II, this issue.

Nishioka, J., Takeda, S., Kudo, I., Tsumune, D., Yoshimura, T., Kuma, K., Tsuda, A., 2003. Size-fractionated iron distributions and iron-limitation processes in the subarctic NW Pacific. Geophysical Research Letters 30 (14), 1730, doi:10.1029/2002GL016853.

Nishioka, J., Ono, T., Saito, H., Nakatsuka, T., Takeda, S., Yoshimura, T., Suzuki, K., Kuma, K., Nakabayashi, S., Tsumune, D., Mitsudera, H., Johnson, W.K., Tsuda, A., 2007. Iron supply to the western subarctic Pacific: Importance of iron export from the Sea of Okhotsk. Journal of Geophysical Research 112, C10012, doi:10.1029/2006JC004055.

Obata, H., Karatani, H., Nakayama, E., 1993. Automated determination of iron in seawater by chelating resin concentration and chemiluminescence detection. Analytical Chemistry 65, 1524–1528.

Oguma, S., Ono, T., Kusaka, A., Kasai, H., Kawasaki, Y., Azumaya, T., 2008. Isotopic tracers for water masses in the coastal region of eastern Hokkaido. Journal of Oceanography 64, 525–539.

Okamoto, S., Hirawake, T., Saitoh, S., Interannual variability of the magnitude and timing of spring bloom in the Oyashio region. Deep-Sea Research II, this issue.

690 Paasche, E., 1980. Silicon content of five marine plankton diatom species measured with a
691 rapid filter method. Limnology and Oceanography 25, 474–480.
692 Price, N.M., 2005. The elemental stoichiometry and composition of an iron-limited diatom.
693 Limnology and Oceanography 50, 1159–1171.
694 Redfield, A.C., Ketchum, B.H., Richards, F.A., 1963. The influence of organisms on the
695 composition of seawater. In: Hill, M.N. (Eds.), The Sea. Vol. 2. Wiley, New York, pp.
696 26–77.
697 Rose, J.M., Caron, D.A., 2007. Does low temperature constrain the growth rates of
698 heterotrophic protists? Evidence and implications for algal blooms in cold waters.
699 Limnology and Oceanography 52, 886–895.
700 Saito, H., Tsuda, A., Kasai, H., 2002. Nutrient and plankton dynamics in the Oyashio region
701 of the western subarctic Pacific Ocean. Deep-Sea Research II 49, 5463–5486.
702 Saito, H., Tsuda, A., 2003. Influence of light intensity on diatom physiology and nutrient
703 dynamics in the Oyashio region. Progress in Oceanography 57, 251–263.
704 Sakurai, Y., 2007. An overview of the Oyashio ecosystem. Deep-Sea Research II 54,
705 2526–2542.
706 Sato, M., Furuya, K., Pico- and nanophytoplankton dynamics during the spring bloom in the
707 Oyashio region. Deep-Sea Research II, this issue.
708 Shinada, A., Ikeda, T., Ban, S., Tsuda, A., 2001. Seasonal dynamics of planktonic food chain
709 in the Oyashio region, western subarctic Pacific. Journal of Plankton Research 23,
710 1237–1247.
711 Silver, M.W., Mitchell, J.G., Ringo, D.L., 1980. Siliceous nanoplankton. II. Newly discovered
712 cysts and abundant choanoflagellates from the Weddell Sea, Antarctica. Marine Biology
713 58, 211–217.
714 Smetacek, V., Passow, U., 1990. Spring bloom initiation and Sverdrup's critical-depth model.
715 Limnology and Oceanography 35, 228–234.
716 Sugie, K., Kuma, K., 2008. Resting spore formation in the marine diatom *Thalassiosira*
717 *nordenskioeldii* under iron- and nitrogen-limited conditions. Journal of Plankton
718 Research 30, 1245–1255, doi:10.1093/plankt/fbn080.
719 Sugie, K., Kuma, K., Fujita, S., Ikeda, T., in press. Increase in Si:N drawdown ratio due to

720 resting spore formation by spring bloom-forming diatoms under Fe- and N-limited
721 conditions in the Oyashio region. Journal of Experimental Marine Biology and Ecology,
722 doi:10.1016/j.jembe.2009.11.001.
723 Suzuki, R., Ishimaru, T., 1990. An improved method for the determination of phytoplankton
724 chlorophyll using N, N-dimethylformamide. Journal of the Oceanographical Society of
725 Japan 46, 190–194.
726 Takahashi, K., Kuwata, A., Saito, H., Ide, K., 2008. Grazing impact of the copepod
727 community in the Oyashio region of the western subarctic Pacific Ocean. Progress in
728 Oceanography 28, 222–240.
729 Takata, T., Kuma, K., Saitoh, Y., Chikira, M., Saitoh, S., Isoda, Y., Takagi, S., Sakaoka, K.,
730 2006. Comparing the vertical distribution of iron in the eastern and western North Pacific
731 Ocean. Geophysical Research Letters 33, L02613, doi:10.1029/2005GL024538.
732 Takeda, S., 1998. Influence of iron availability on nutrient consumption ratio of diatoms in
733 oceanic waters. Nature 393, 774–777.
734 Taniguchi, A., 1999. Difference in the structure of the lower trophic levels of pelagic
735 ecosystem in the eastern and western subarctic Pacific. Progress in Oceanography 43,
736 289–315.
737 Taniguchi, A., Suzuki, T., Shimada, S., 1995. Growth characteristics of Parmales
738 (Chrysophyceae) observed in bag culture. Marine Biology 123, 631–638.
739 Thompson, P.A., Levasseur, M.E., Harrison P.J., 1989. Light-limited growth on ammonium vs.
740 nitrate: What is the advantage for marine phytoplankton? Limnology and Oceanography
741 34, 1014–1024.
742 Thompson, R.J., Deibel, D., Redden, A.M., McKenzie, C.H., 2008. Vertical flux and fate of
743 particulate matter in a Newfoundland fjord at sub-zero water temperatures during spring.
744 Marine Ecology Progress Series 357, 33–49.
745 Tsuda, A., Takeda, S., Saito, H., Nishioka, J., Nojiri, Y., Kudo, I., Kiyosawa, H., Shiomoto, A.,
746 Imai, K., Ono, T., Shimamoto, A., Tsumune, D., Yoshimura, T., Aono, T., Hunuma, A.,
747 Kinugasa, M., Suzuki, K., Sohrin, Y., Noiri, Y., Tani, H., Deguchi, Y., Tsurushima, N.,
748 Ogawa, H., Fukami, K., Kuma, K., Saino, T., 2003. A mesoscale iron enrichment in the
749 western subarctic Pacific induces a large centric diatom bloom. Science 300, 958–961.

Tsurushima, N., Nojiri, Y., Imai, K., Watanabe, S., 2002. Seasonal variations of carbon dioxide system and nutrients in the surface mixed layer at station KNOT (44°N, 155°E) in the subarctic western North Pacific. Deep-Sea Research II 49, 5377–5394.

Welschmeyer, N.A., 1994. Fluorometric analysis of chlorophyll *a* in the present of chlorophyll *b* and pheopigments. Limnology and Oceanography 39, 1985–1992.

Wong, C.S., Waser, N.A.D., Nojiri, Y., Whitney, F.A., Page, J.S., Zeng, J., 2002. Seasonal cycles of nutrients and dissolved inorganic carbon at high and mid latitudes in the North Pacific Ocean during the *Skaugran* cruises: determination of new production and nutrient uptake ratios. Deep-Sea Research II 49, 5317–5338.

780 **Table and Figure captions**

781

782 Table 1. Cast, sampling date and measurements. Abbreviations; CTD:
783 conductivity-temperature-depth, Nuts: nutrients, NO_3+NO_2, PO_4 and $Si(OH)_4$, Fe:
784 dissolved Fe (<0.22 μm) and total Fe (unfiltered), Chl: chlorophyll *a*, and BSi: biogenic
785 silica. Initials in cast numbers, OS and KH, indicates Oshoro-maru and Hakuho-maru
786 cruises, respectively.

787 Table 2. D-Fe and T-Fe concentrations and nutrient utilization per unit Chl-*a* increment in the
788 each of the culture experiments. Data for ΔNutrients/ΔChl-*a* represent the means of
789 triplicate bottles ± 1SD.

790

791 Fig. 1. Temporal variations in (a) temperature, (b) salinity, (c) sigma-*t*, and (d) Chl-*a* in the
792 upper 150 m. Experiments were conducted aboard the TS Oshoro-Maru from 8- to
793 14-March 2007, and the RV Hakuho-Maru from 5-April to 2-May 2007. Four storms
794 prevented sampling during 11- to 13-March, 14- to 15-April, 21- to 22-April, and 27- to
795 28-April.

796 Fig. 2. The relationships temperature versus *in situ* nutrients of (a) N+N, (b) P and (c) Si in
797 the upper 150 m of the water column. Filled and open symbols represent the nutrient
798 concentrations below the MLD and in the upper mixed layer, respectively.

799 Fig. 3. The relationships of temperature versus *in situ* nutrient ratios for (a) (N+N):P, (b) Si:P,
800 and (c) Si:(N+N) in the upper 150 m of the water column. Dashed line represents
801 Redfield ratio of (a) N:P = 16, (b) Si:P = 15, and (c) Si:N = 0.93 (Redfield et al., 1963;
802 Brzezinski, 1985). Filled and open symbols represent the ratios of macronutrients below
803 the MLD and in the upper mixed layer, respectively.

804 Fig. 4. The relationships between temperature and (a) D-Fe, and (b) T-Fe in the upper 150 m
805 of the water column. Filled and open symbols represent the iron concentrations below
806 the MLD and in the upper mixed layer, respectively.

807 Fig. 5. Vertical profiles of NH_4 and Chl-*a*. (a) Pre-bloom of OS07005 (9-March) and
808 OS07006 (10-March), (b) KH07c012 (8-April) and KH07c026 (12-April), and (c)
809 KH07c054 (24-April) and KH07c057 (25-April).

Fig. 6. The relationship between Chl-*a* and (a) upper mixed layer (closed circle) and below the MLD (open diamond) of BSi, and (b) upper mixed layer BSi, distinguishing the data from <4°C (open circle) and >4°C (closed circle). The figure inserted in (a) expands the ranges from 0 to 1 μg L^{-1} for Chl-*a* and 0 to 2 μmol L^{-1} for BSi. The plotted lines in (b) were obtained by least-squares regression: $[BSi]_{<4°C}$ (μmol L^{-1}) = (1.15 ± 0.14) × [Chl-*a*] + 18.0 (r^2 = 0.93, n = 7, p<0.001) and $[BSi]_{>4°C}$ (μmol L^{-1}) = (2.14 ± 0.08) × [Chl-*a*] + 6.9 (r^2 = 0.94, n = 43, p<0.001). Dashed lines indicate 95% confidence limits of the regression.

Fig. 7. Temporal changes in (a) Chl-*a*, (b) N+N, (c) P and (d) Si during the culture experiments. Data are represented as the means ± 1SD of triplicate bottles.

Fig. 8. The relationships between the warmer Modified Kuroshio Water (MKW) mixing ratio and estimated macronutrient concentrations during winter for (a) $[N+N]_{winter}$, (b) $[P]_{winter}$ and (c) $[Si]_{winter}$, and (d) the ratios of $[N+N]_{winter}$:$[P]_{winter}$, $[Si]_{winter}$:$[P]_{winter}$ and $[Si]_{winter}$:$[N+N]_{winter}$ calculated from the regressions of Fig. 8a–c. The MKW ratio represents the contribution of MKW to MKW + Coastal Oyashio Water + Oyashio Water (Kono and Sato, this issue). The plotted lines were obtained by least-squares regression for (a) $[N+N]_{winter}$ (μmol L^{-1}) = (–13.3 ± 1.2) × (MKW ratio) + 18.7 (r^2 = 0.70, n = 50, p<0.001), (b) $[P]_{winter}$ (μmol L^{-1}) = (–1.14 ± 0.09) × (MKW ratio) + 1.89 (r^2 = 0.77, n = 50, p<0.001), and (c) $[Si]_{winter}$ (μmol L^{-1}) = (–38.0 ± 5.1) × (MKW ratio) + 43.6 (r^2 = 0.53, n = 50, p<0.001). Dashed lines indicate 95% confidence limits of the regression. The thin line in (d) represents the approximate Redfield ratio (Redfield et al., 1963; Brzezinski, 1985).

Fig. 9. The relationship of Chl-*a* concentration at 5 m and (a) mixed layer depth (MLD, m), (b) temperature, (c) T-Fe, (d) N+N and (e) D-Fe, and (f) temperature at 5 m and MLD. The plotted line was obtained by least-square regression: (a) [Chl-*a*] (μg L^{-1}) = 290 × $MLD^{-1.17}$ (r^2 = 0.86, n = 19, p<0.001), (b) [Chl-*a*] (μg L^{-1}) = –2.79 × T (°C) + 16.6 (r^2 = 0.75, n = 19, p<0.001), (c) [Chl-*a*] (μg L^{-1}) = 0.63 × [T-Fe] (nmol L^{-1}) + 0.57 (r^2 = 0.74, n = 19, p<0.001), (d) [Chl-*a*] (μg L^{-1}) = –0.74 × [N+N] (μmol L^{-1}) + 11.1 (r^2 = 0.31, n = 19, p<0.05), and (f) MLD = 5.56 × $e^{0.514 \times T (°C)}$ (r^2 = 0.73, n = 19, p<0.001). No significant relationship among [D-Fe] and [Chl-*a*] (e).

Table 1. Cast, sampling date and measurements. Abbreviations; CTD: conductivity-temperature-depth, Nuts: nutrients, NO_3+NO_2, PO_4 and $Si(OH)_4$, Fe: dissolved Fe (<0.22 μm) and total Fe (unfiltered), Chl-*a*: chlorophyll *a*, and BSi: biogenic silica. Initial of cast numbers of OS and KH indicates Oshoro-maru and Hakuho-maru cruise, respectively.

Cast	Date	Measurement
OS07005	09/03/2007	CTD, Nuts, Fe, Chl-*a*, BSi, Culture (March)
OS07006	10/03/2007	CTD, Nuts, Fe, Chl-*a*, BSi
OS07008	14/03/2007	CTD, Nuts, Fe, Chl-*a*, BSi
KH07c005	06/04/2007	CTD, Nuts, Fe, Chl-*a*, BSi, Culture (6-Apr)
KH07c008	07/04/2007	CTD, Nuts, Fe, Chl-*a*
KH07c012	08/04/2007	CTD, Nuts, Fe, Chl-*a*
KH07c020	10/04/2007	CTD, Nuts, Fe, Chl-*a*
KH07c026	12/04/2007	CTD, Nuts, Fe, Chl-*a*, BSi
KH07c029	13/04/2007	CTD, Nuts, Fe, Chl-*a*
KH07c033	16/04/2007	CTD, Nuts, Fe, Chl-*a*
KH07c037	17/04/2007	CTD, Nuts, Fe, Chl-*a*, BSi
KH07c041	18/04/2007	CTD, Nuts, Fe, Chl-*a*
KH07c045	19/04/2007	CTD, Nuts, Fe, Chl-*a*, BSi
KH07c048	20/04/2007	CTD, Nuts, Fe, Chl-*a*, Culture (20-Apr)
KH07c054	24/04/2007	CTD, Nuts, Fe, Chl-*a*
KH07c057	25/04/2007	CTD, Nuts, Fe, Chl-*a*
KH07c061	26/04/2007	CTD, Nuts, Fe, Chl-*a*, BSi
KH07c067	30/04/2007	CTD, Nuts, Fe, Chl-*a*, BSi
KH07c070	01/05/2007	CTD, Nuts, Fe, Chl-*a*

Table 2. D-Fe and T-Fe concentrations and nutrient utilization per unit Chl-*a* increment of the each culture experiments. Data for ΔNutrients/ΔChl-*a* represent the means of triplicate bottles ± 1SD.

Experiment	Temperature (°C)	D-Fe (nmol L^{-1})	T-Fe (nmol L^{-1})	ΔN/ΔChl *a*	ΔP/ΔChl *a*	ΔSi/ΔChl *a*
March	6.2	0.38	3.57	0.81 ± 0.20	0.084 ± 0.059	0.24 ± 0.35
6-April	1.7	0.41	15.70	1.32 ± 0.11	0.058 ± 0.008	0.96 ± 0.09
20-April	3.6	0.17	3.38	2.69 ± 0.18	0.113 ± 0.009	3.29 ±0.36

Fig. 1

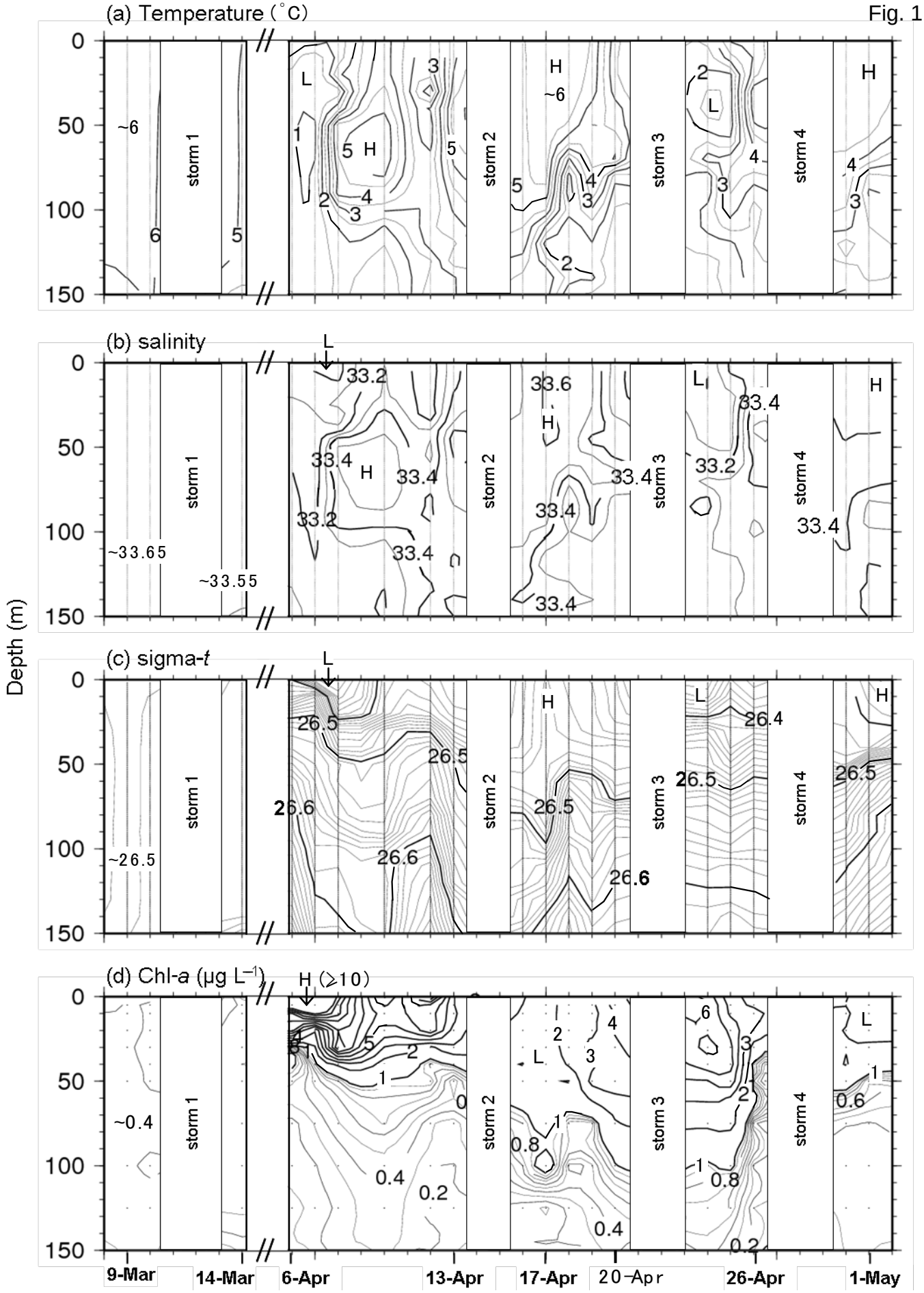
(a) Temperature (°C)
(b) salinity
(c) sigma-t
(d) Chl-a (μg L⁻¹)
Depth (m)
storm 1
storm 2
storm 3
storm 4
9-Mar
14-Mar
6-Apr
13-Apr
17-Apr
20-Apr
26-Apr
1-May

Fig. 2

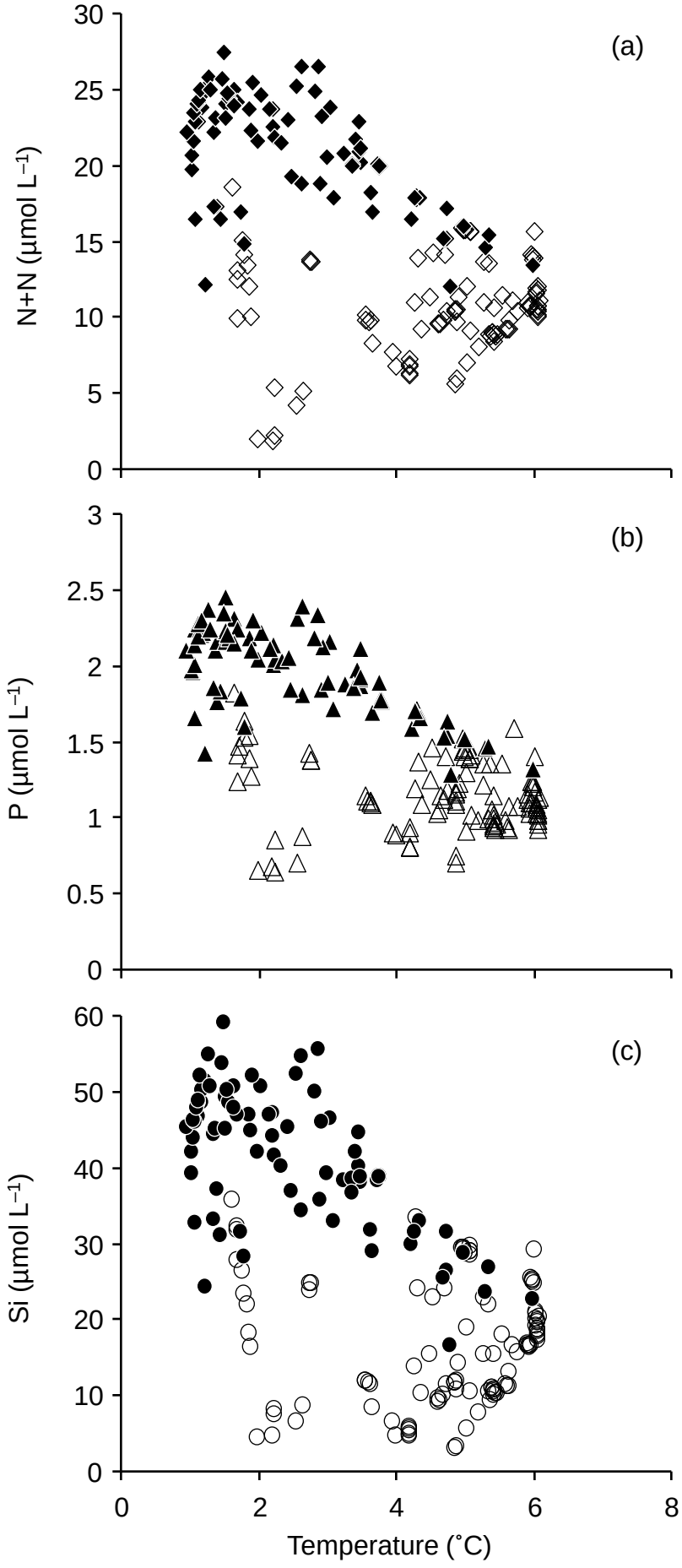
(a)
N+N (µmol L⁻¹)
30
25
20
15
10
5
0
(b)
P (µmol L⁻¹)
3
2.5
2
1.5
1
0.5
0
(c)
Si (µmol L⁻¹)
60
50
40
30
20
10
0
0
2
4
6
8
Temperature (˚C)

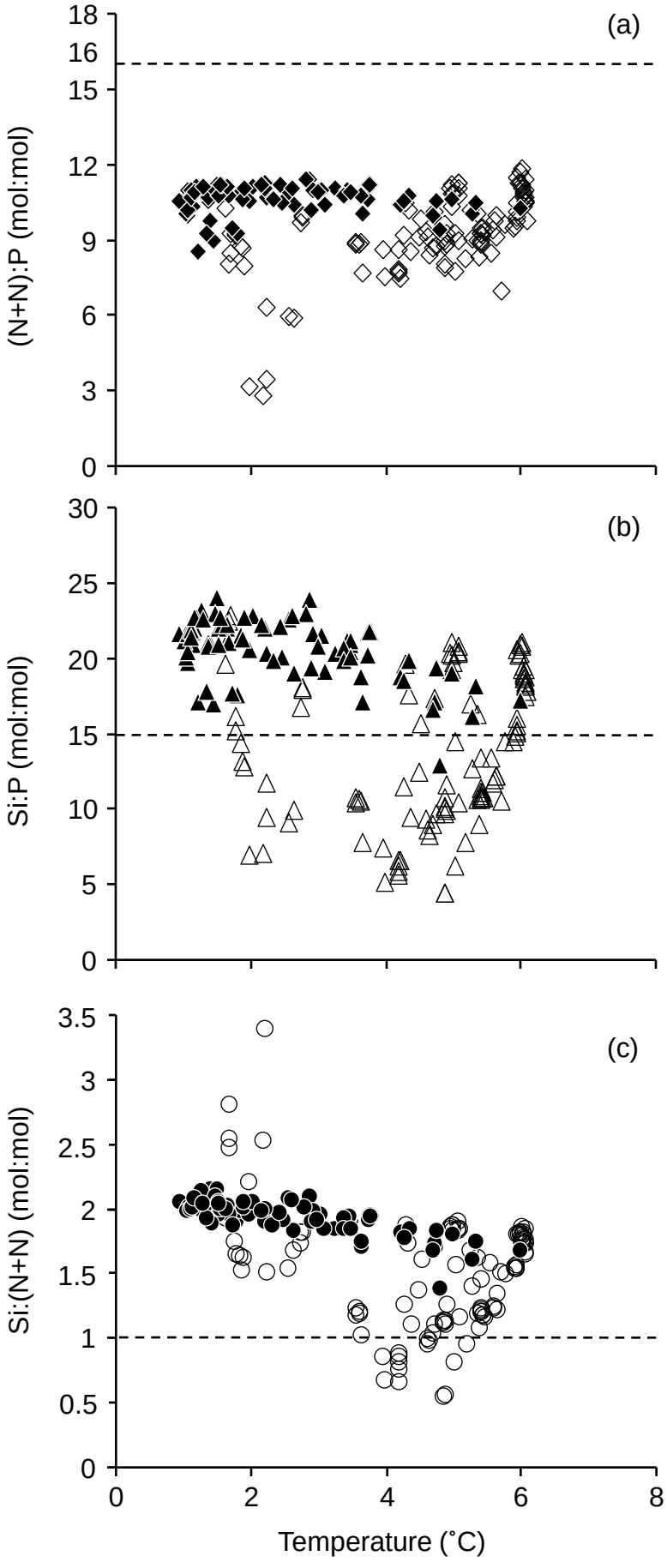
(a)
(N+N):P (mol:mol)
18
16
15
12
9
6
3
0
(b)
Si:P (mol:mol)
30
25
20
15
10
5
0
(c)
Si:(N+N) (mol:mol)
3.5
3
2.5
2
1.5
1
0.5
0
0
2
4
6
8
Temperature (˚C)

Fig. 4

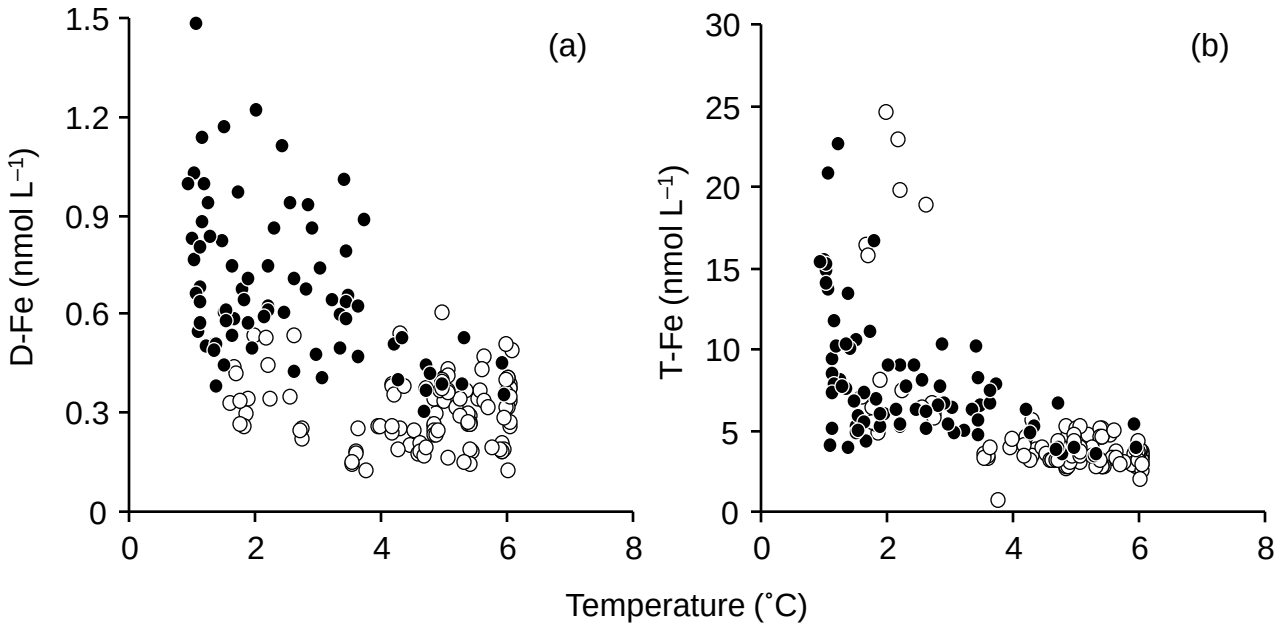
(a)
(b)
D-Fe (nmol L⁻¹)
T-Fe (nmol L⁻¹)
Temperature (˚C)
0
0.3
0.6
0.9
1.2
1.5
5
10
15
20
25
30
2
4
6
8

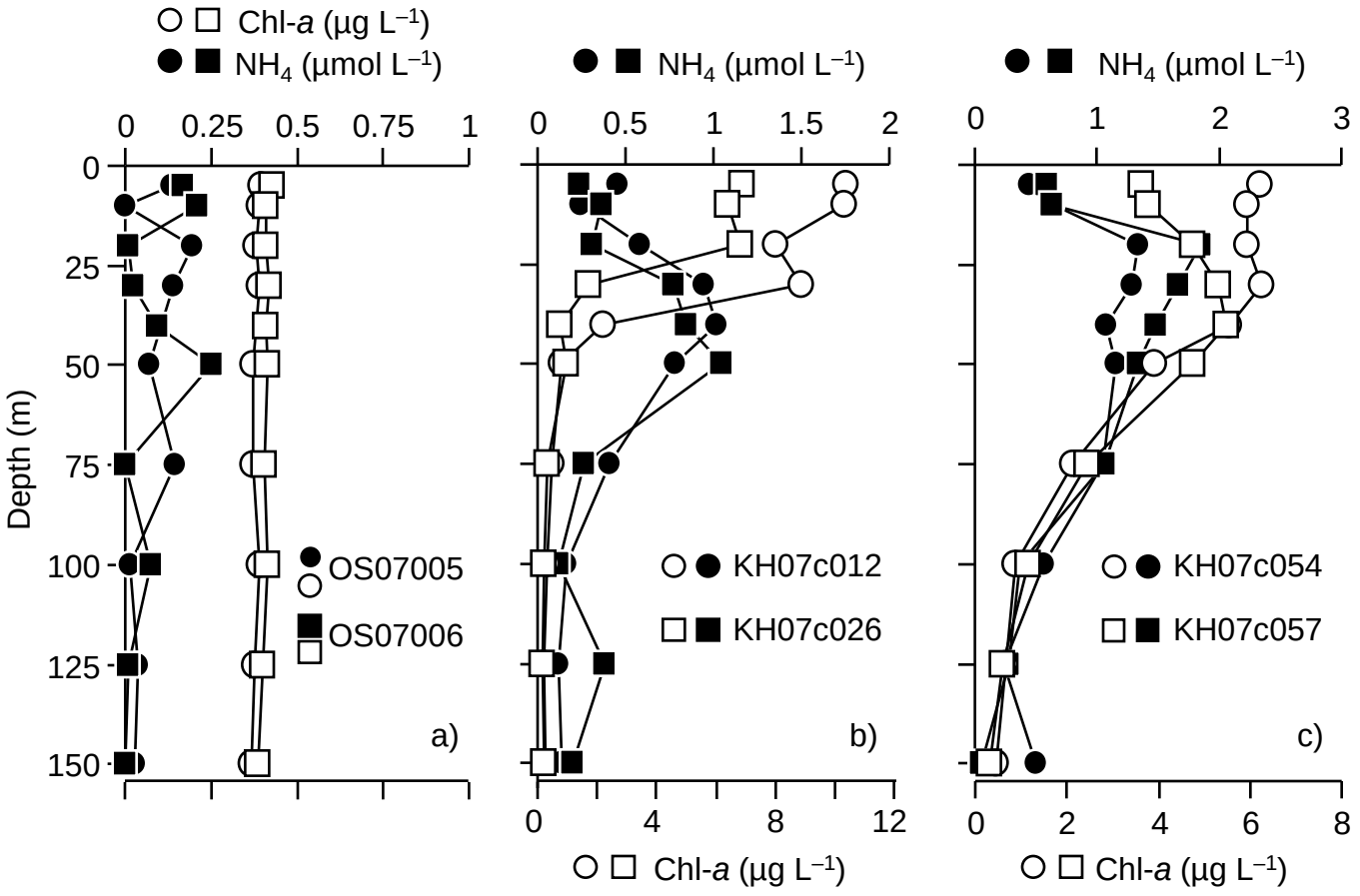
Chl-a (µg L−1)
NH4 (µmol L−1)
Depth (m)
0
25
50
75
100
125
150
0
0.25
0.5
0.75
1
OS07005
OS07006
a)
0
0.5
1
1.5
2
KH07c012
KH07c026
b)
0
4
8
12
0
1
2
3
KH07c054
KH07c057
c)
0
2
4
6
8

Fig. 6

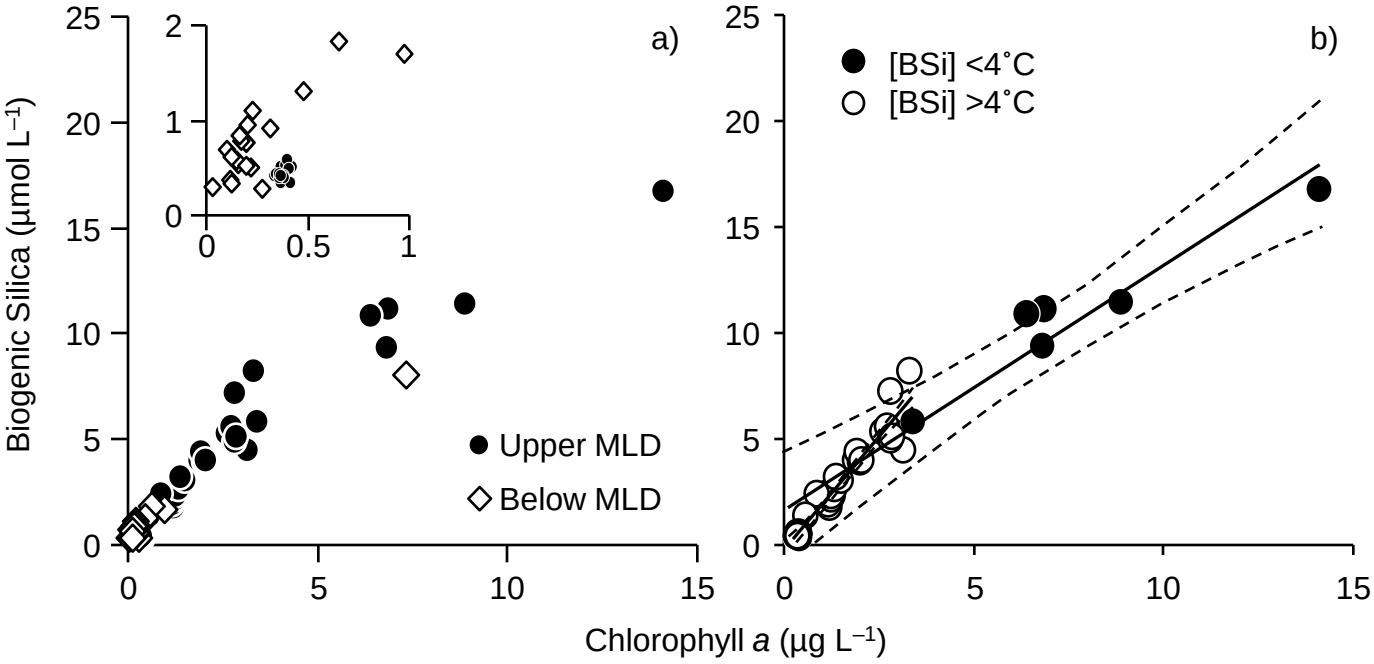
a)
b)
Biogenic Silica (µmol L⁻¹)
Chlorophyll a (µg L⁻¹)
Upper MLD
Below MLD
[BSi] <4˚C
[BSi] >4˚C
0
5
10
15
20
25
0.5
1
2

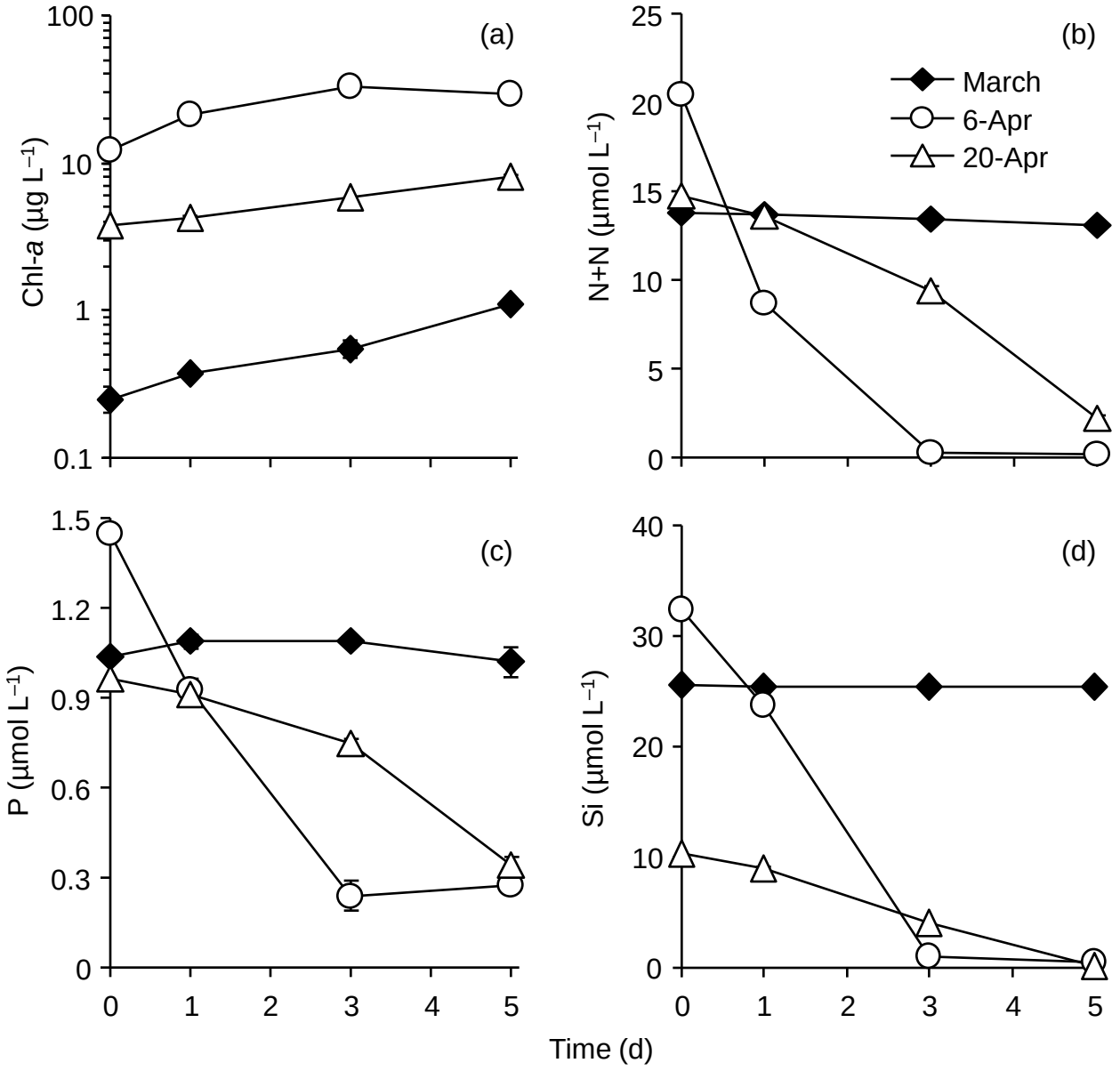
(a)
Chl-a (µg L⁻¹)
100
10
1
0.1
(b)
N+N (µmol L⁻¹)
25
20
15
10
5
0
March
6-Apr
20-Apr
(c)
P (µmol L⁻¹)
1.5
1.2
0.9
0.6
0.3
0
(d)
Si (µmol L⁻¹)
40
30
20
10
0
0 1 2 3 4 5
Time (d)

Fig. 8

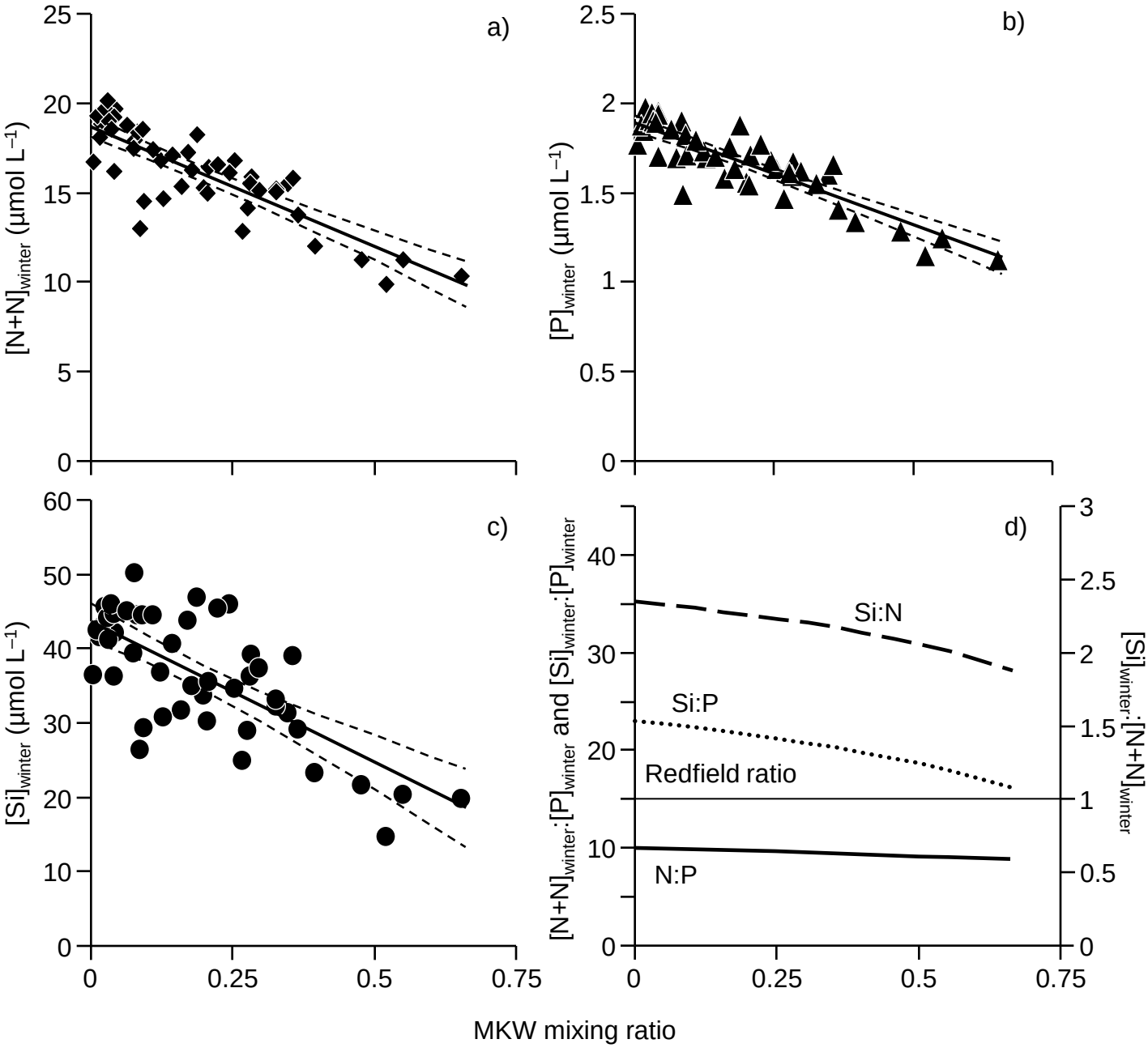
a)
b)
c)
d)
[N+N]winter (µmol L−1)
[P]winter (µmol L−1)
[Si]winter (µmol L−1)
[N+N]winter:[P]winter and [Si]winter:[P]winter
[Si]winter:[N+N]winter
Si:N
Si:P
Redfield ratio
N:P
MKW mixing ratio

Fig. 9

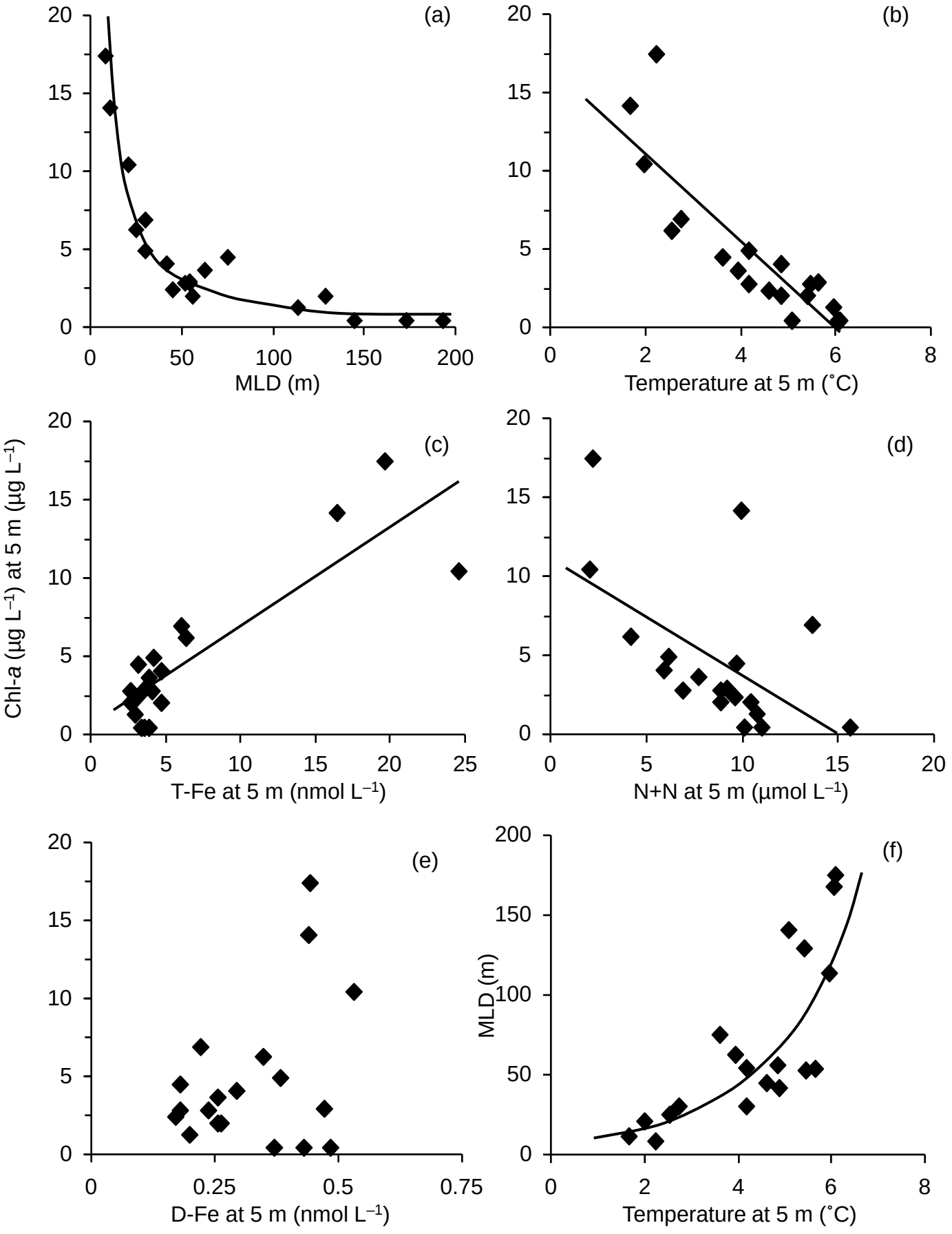
(a)
MLD (m)
(b)
Temperature at 5 m (˚C)
(c)
Chl-a (µg L–1) at 5 m (µg L–1)
T-Fe at 5 m (nmol L–1)
(d)
N+N at 5 m (µmol L–1)
(e)
D-Fe at 5 m (nmol L–1)
(f)
MLD (m)
Temperature at 5 m (˚C)